Turkish Journal of Physics

http://journals.tubitak.gov.tr/physics/

Research Article

Turk J Phys
(2017) 41: 426 – 435

doi:10.3906/fiz-1704-9

Proton–proton and proton–antiproton differential elastic cross sections modeling at high and ultra-high energies using a hybrid computing paradigm

EL-Sayed EL-DAHSHAN[1,2,*]
[1]Department of Physics, Faculty of Sciences, Ain Shams University, Abbassia, Cairo, Egypt
[2]Egyptian E-Learning University (EELU), Eldoki, El-Geiza, Egypt

Received: 10.04.2017 • **Accepted/Published Online:** 18.08.2017 • **Final Version:** 10.11.2017

Abstract: This work presents a hybrid computing technique for modeling the differential elastic cross section of both proton–proton "pp" and proton–antiproton "pp(bar)" collisions from high to ultra-high energy regions (from 13.9 GeV to 14 TeV) as a function of the center-of-mass energy "s" squared and four momentum transfer squared "t". We proposed a genetic algorithm (GA) and support vector regression (SVR) hybrid techniques to calculate and predict the "differential elastic cross section" of both "pp" and "pp(bar)". Our proposed GA-SVR hybrid model shows a good match to the available experimental data, as well as predicting the latest and future "TOTEM" experiments for differential elastic cross sections that are not utilized in the training phase. An extrapolation of the differential cross section to $|t| \rightarrow 0$ gives the total cross section through the optical theorem. The model calculations and predictions for "pp" and "pp(bar)" total cross-sections over a wide collision energy ranging from ISR to LHC are given. All the results for the total cross-sections matched well with the last and the more recent measurements ($\sqrt{s}$= 7 TeV and 8 TeV), as well as the results of other models for the future "TOTEM" measurements at ($\sqrt{s}$ = 10 TeV and 14 TeV).

Key words: Deferential elastic cross sections, proton–proton (antiproton) collision, empirical modeling, support vector regression, genetic algorithm

1. Introduction

Proton–proton (pp) and proton-antiproton ($P\overline{P}$) cross sections at high energy are the first studies performed when a new hadron accelerator opens up a new energy region. The study of the total PP and $P\overline{P}$ cross section and its various subcomponents (elastic, inelastic, and diffractive) is a very powerful tool to understand the strong interaction mechanism [1–6]. Elastic pp and $p\bar{p}$ scattering is the most essential component in high energy hadronic interactions to investigate the structure of the proton [7]. There are three important physical components to characterize the elastics pp and $p\bar{p}$ scattering: total cross section "$\sigma_{tot}^{pp,\ p\bar{p}}$", differential cross section "$\left(\frac{d\sigma}{dt}\right)^{pp,\ p\bar{p}}$", and the ratio of the forward real to imaginary parts of the elastic scattering amplitude "ρ-parameter" [8]. The elastic differential cross section of PP and $P\overline{P}$ contains information about proton structure and nonperturbative aspects of PP and $P\overline{P}$ interactions, as well as providing useful information on the behavior of the scattering amplitude, in particular, on the nature of their diffractive components [9]. The "total cross section" $\sigma_{tot}^{pp,\ p\overline{p}}$ can be obtained from the calculation of elastic scattering ones depending on the

*Correspondence: e_eldahshan@yahoo.com

"optical theorem" [10,11]. The investigation of high energy PP and $P\overline{P}$ elastic cross section depends mainly on the "center of mass energy" ($\sqrt{s}$) and the "four-momentum transfer squared" (t) [1–5].

The high energy PP and $P\overline{P}$ elastic scattering have been measured experimentally at different colliders over a wide range of $\sqrt{s}_{,\,such\,as}$ "Intersecting Storage Rings (ISR)" and "Super Proton Synchrotron (SPS)" colliders at the "European Council for Nuclear Research (CERN)" [12–20], as well as the "Fermilab" fixed target experiments and Tevatron colliders [21–29]. Recently, the measurements of the high energy PP and $P\overline{P}$ elastic scattering have been working at the Large Hadron Collider "LHC" by the "TOTEM" (TOTal cross section, Elastic scattering and diffraction dissociation Measurement) at the LHC Collaboration [30–35]. Furthermore, different theoretical models have been proposed to investigate the PP and $P\overline{P}$ elastic scattering; most of them are QCD-based models [9]. This wide array of experimental and theoretical models attempt to describe pp elastic scattering at LHC. In addition, the understanding of this process will provide fundamental insight into the nonperturbative and the perturbative QCD [7,9]. To our knowledge, despite the amount of available experimental data and model descriptions of these data, a precise and complete description of differential and total cross sections is still lacking and this issue is an open issue. Considering that, we hope our model may bring insights for further and deeper developments.

In recent years, the artificial neural networks (ANNs) [36] approach has been widely used for prediction of physics as classification and regression problems [37–42]. However, this approach has been found to be more efficient compared to statistical algorithms. It has many downsides such as over-fitting, slow convergence, and less generalizing performance. Support vector machine (SVM) is a machine-learning algorithm developed by Vapnik (1995) to solve regression problems [43]. The SVMs also have been modified to the so-called support vector regression (SVR) for manipulating nonlinear regression estimation problems [43–45]. Thus, the process of applying SVMs in regression problems is referred to as SVR. However, it is necessary to optimize the SVM parameters. Appropriate parameters in SVR lead to overfitting or underfitting. Therefore, selecting optimal hyperparameters is an important step in SVR design. Genetic algorithms (GAs) are search algorithms based upon the mechanics of natural selection [46,47]. In this study, we propose a GA to determine parameters of SVR that optimizes all SVR's parameters simultaneously from the training data. Thus, the aim of this article is to suggest a hybrid model GA-SVR to calculate and predict the "$\left(\frac{d\sigma}{dt}\right)^{pp,\,p\overline{p}}$" as a function of "$\sqrt{s}$" and "$|t|$", as well as "$\sigma_{tot}^{pp,\,p\overline{p}}$" at various $\sqrt{s}$ ranging from nearly $\sqrt{s} = 13.9$ GeV to $\sqrt{s} = 14$ TeV for $|t| = 0$ to 6 GeV^2.

The next sections of this paper are structured as follows: Section 2 presents the proposed GA-SVR to model the PP and $P\overline{P}$ deferential elastic cross sections. The results obtained are explained in Section 3. Lastly, Section 4 provides the findings and conclusions.

2. The proposed hybrid GA-SVR model

Creating an accurate mathematical model that can simulate and predict the nonlinear behavior of physical phenomena is a challenging issue. In the present study, we developed a hybrid soft computing approach GA-SVR based on experimental data to calculate and predict the differential elastic cross section of both PP and $P\overline{P}$ collisions, $\left(\frac{d\sigma}{dt}\right)^{pp,\,p\overline{p}}$, i.e. $\frac{d\sigma}{dt} = f\left(\sqrt{s},\, t\right)$ as well as $\sigma_{tot}^{pp,\,p\overline{p}}$. The following subsections describe the development of our hybrid computing GA-SVR model for calculating and predicting of the $\left(\frac{d\sigma}{dt}\right)^{pp,\,p\overline{p}}$ and $\sigma_{tot}^{pp,\,p\overline{p}}$.

2.1. Mathematical formulation of support vector regression

SVM was invented in 1992 by Vapink et al. [43–45] as a classification tool and was extended to a nonlinear regression case "support vector regression (SVR)" in 1997 [43–45]. SVR is a powerful function approximation approach based on statistical learning theory. Using the so-called ε-insensitive loss function for SVR (ε-SVR), we ensure the finding of the global minimum and the optimization of the generalization error over the parameter space.

In SVR, the given training set is $\{(x_i, y_i),\ i = 1, ...,\ell\} \subset R^d \times R$, *where* $x_i \in R^d$ is the ith input vector in the "input space x", y_i is the corresponding ith output (in our case x_1 denotes the center of mass energy $(\sqrt{s})$ and the four – momentum transfer squared (t), y_i denotes the differential cross section for PP and $P\overline{P}$ collisions " $\left(\frac{d\sigma}{dt}\right)^{pp,\, p\bar{p}}$ "; the input space x is first mapped onto high-dimensional "feature space" using nonlinear mapping function (kernel function $g(x)$) and then a linear model is constructed in this feature space to estimate the output y_i using the SVR regression function $f(x) = w\, g(x) + b; w$ and b are the "weight" vector and the "bias" term, respectively. Using mathematical notation, the generic linear SVR approximator $f(x,\, w)$ in the high-dimensional feature space is defined as follows:

$$\frac{d\sigma}{dt} = f(x,\, w) = f\left(\sqrt{s},\, t,\, w\right) = \sum\nolimits_{j=1}^{m} w_i g_j\,(x) + b, \tag{1}$$

where $g_j\,(x)\,, \quad j = 1, ..., m$ denotes a set of nonlinear transformations (mapping function), and w and b are the "weight" vector and the "bias" term, respectively.

The quality of estimation of the ε-SVR regression model is measured by a new type of loss function called ε-insensitive loss function proposed by Vapnik [43–45]. ε-SVR performs linear regression in the high-dimension feature space using ε-insensitive loss and, at the same time, tries to reduce model complexity by minimizing $\frac{1}{2}\ \|w\|^2$ (norm of the weights vector), which is subject to $y_i(w^T x_i + b) \geq 1$. This is an optimization problem, which can be converted to the dual optimization problem. Therefore, the regression function (the estimated function of the output, y_i, in our case is $\frac{d\sigma}{dt}$) "eqn 1" can be rewritten as a generic function and is given by

$$f(x_i, \alpha^*, \alpha) = \sum_{i=1}^{n_{SV}} (\alpha_i - \alpha_i^*) K(x_i, x) + b$$

$$0 \leq \alpha_i,\, \alpha_i^* \leq C\ (C\ \text{is penalty parameter}) \text{ and } \sum_{i=1}^{N} (\alpha_i - \alpha_i^*) = 0 \tag{2}$$

where "n_{SV}" is the number of Support Vetors "SV_s"

The Lagrange multipliers of the dual optimization problem, α_i, α_i^* are obtained and then w and b are given as $\omega = \sum\limits_{i=1}^{l} (\alpha_i - \alpha_i^*) x$ and $b = -\frac{1}{2} \left\langle \omega, (x_p + x_s) \right\rangle$, where x_r and x_s are any support vectors and $k\,(x_i,\, x_j) = (g\,(x_i)\ .\, g\,(x_j))$ is the kernel function. The kernel function used in the study is a (Gaussian kernel) radial basis function (RBF), $k(x_i,\ x_j) = \exp\left(-\gamma ||x_i - x_j^*||^2\right)$, where x_i and x_j are inner vectors in the input space and γ is a parameter that sets the "spread" of the kernel.

According to the above short overview of the SVR, $(C,\, \gamma,\, \varepsilon)$ are the most important parameters of the SVR approach. All these parameters are considered for calculating and predicting the new output based on

any new input features and they are user-defined parameters. Various methods are proposed for selecting these parameters automatically. In this study, the evolutionary GA is utilized to select the optimal parameters of the SVR model to achieve a better generalization performance of the hybrid (GA-εSVR) model.

2.2. Genetic algorithm approach

GAs are stochastic search techniques based on the Darwinian principle of natural selection, "survival of the fittest", and genetics gained attention after Holland in 1975 [46]. The GA method has three basic evolutionary operators, "reproducing operators": selection, crossover, and mutation. Based on these operators, the GA begins from a randomly made up population of individuals (chromosomes/solutions), which are expressed as a "genotype". For each generation, the fitness of chromosomes is evaluated based on a fitness function [46,47]. The size of the population and the probability for crossover and mutation are called the control parameters of the GA. The solution in the real world is known as a "phenotype". The genotype is transformed into the phenotype for the fitness evaluation process. For more information about the GA, please see Ref. [46].

2.3. Workflow of the GA-SVR model

To build and train our GA-SVR approach for calculation and prediction of differential elastic cross section $\left(\frac{d\sigma}{dt}\right)^{pp,\,p\bar{p}}$, the available experimental datasets [11–35] are randomly divided into two subsets, one for training and the other for testing the GA-SVR model. We apply 5-fold cross-validation accuracy computing by SVR on the training data set (experimental data) to the GA-fitness function. The training dataset is used to obtain the SVR parameters and radial basis function (RBF) width parameter $(C,\,\gamma,\,\varepsilon)$. The testing data are utilized to investigate the prediction performance of the model. At first, the training inputs and outputs, range of the SVR and RBF parameters, population size, and number of generations are fed to the GA. Then the initial population is generated in the GA. Moreover, 5-fold cross validation is used for avoiding the problem of overfitting during the training and obtaining the best fitness values. The fitness value (mean squared error (MSE)) is obtained for each individual of the population. This procedure is repeated until all individuals (candidate solutions) are evaluated. After that, a new population is generated using genetic operators, i.e. selection, crossover, and mutation operators. Generation of the new populations continues for 50 times. The genetic operators, one point crossover, and mutation are used. The crossover rate is 90% and mutation rate is 10%. The Tournoi selection method is used to select the mating pool. The optimal SVR parameters $(C,\,\gamma,\,\varepsilon)$ are obtained to learn the model. Then the optimal parameters are chosen using the individual with the best fitness value at the last generation. The final evaluation of the model performance is the testing based on the unseen experimental data. The criteria of root mean square (MSE) and coefficient of determination (R^2) were used for evaluating the performance of the GA-SVR models [48]. The developed model GA-εSVR is used to predict $\left(\frac{d\sigma}{dt}\right)^{pp,\,p\bar{p}}$ in this study. The basic flowchart of the GA-εSVR model is depicted in Figure 1. The proposed hybrid GA-SVR model was developed and implemented in the MATLAB v6.5 environment with high degree of accuracy and reliability.

3. Results and discussion

We have applied the developed hybrid computing approach using GA and ε-SVR to reasonably reproduce and calculate the differential elastic cross section based on the existing experimental data for PP and $P\overline{P}$ scattering, as described in the above section. The available experimental data are collected from a set of accelerators in a

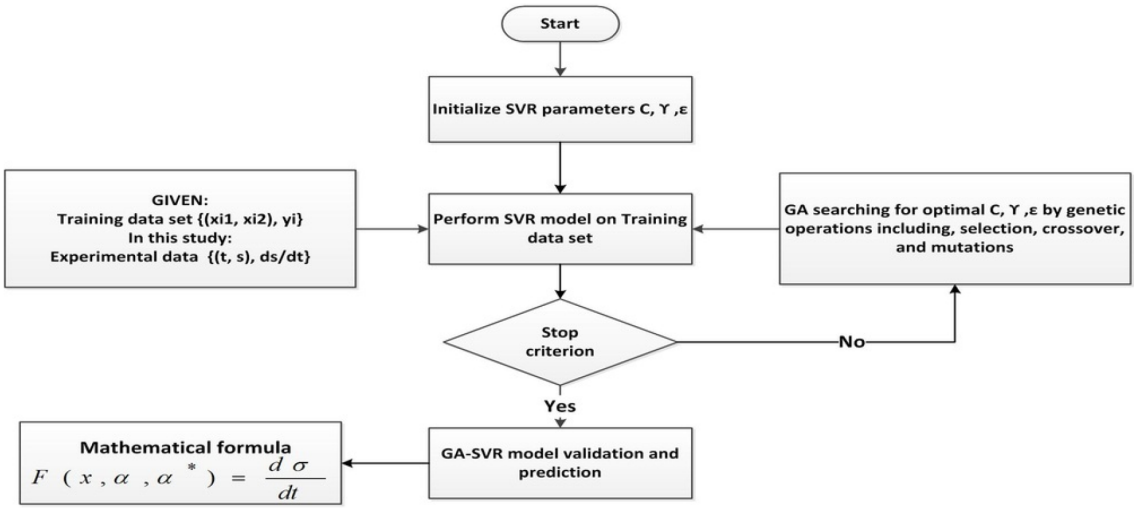

Figure 1. Flow diagram of our GA-εSVR model.

wide energy range from ISR energy range up to the LHC, including 14, 23.5. 30.7, 44.6, 52.8-, 62 GeV, as well as the recent LHC energies 7 and 8 TeV (CMS preliminary) for pp scattering [11–35] and 14, 53, 546 GeV, and 1.800 TeV for $P\overline{P}$ scattering [12–35]. These datasets cover the momentum transfer range $0 < \mathrm{t} < 6$ GeV^2.

The available experimental studies covering $\sqrt{s}$ range from 23 to 62 GeV at ISR to 2 TeV at Tevatron, as well as 7 and 8 TeV. At LHC, pp elastic differential cross section is planned to be measured at the unprecedented $\sqrt{s}$ of 14 TeV by the experimental group TOTEM in the "$|t|$" range $0 > \mathrm{t} > 6$ GeV2 .

Figure 2 (a and b) illustrates the dependence of differential elastic cross section $\left(\frac{d\sigma}{dt}\right)^{pp,\, p\bar{p}}$ on $|t|$, which shows a sharp peak at small values of $|t|$ ranging from 0.01 to 0.5 GeV^2 and after this range the differential elastic cross section decreases exponentially to a dip at about $|t| = 1.4$ GeV^2. In addition, from this figure, we note that after $|t| = 1.4$ GeV^2 the differential elastic cross section manifests a broad maximum around $|t| = 2$ GeV^2 and then gradually decreases. Moreover, the obtained results confirm that the strong peak at low $|t|$ seems to become smaller with the increase in energy; in addition, the dip moves towards lower values of $|t|$. This confirms the behavior observed from the previous different experimental and theoretical studies [11–35,49,50]. In addition, the comparison between the experimental and other theoretical models is shown in Figure 2. In this comparison, our model calculations are highly matched with the theoretical and experimental ones.

We have used our model to predict the differential elastic pp cross section at $\sqrt{s} = 10$, 13 (CMS preliminary), and 14 TeV. These predicted values are compared with other models [49,50] as shown in Figure 3. Figure 3 shows a good agreement between our model results and other theoretical ones [49,50].

For the sake of completeness, we applied the proposed GA-SVR model to the pp scattering data. We proceeded in the same manner as previously mentioned for pp scattering, using the SPS and Tevatron experimental data. Figure 4 demonstrates the calculated differential elastic cross section of $P\overline{P}$ scattering at $\sqrt{s}$=14, 53, 546 GeV, and 1.800 TeV. For $P\overline{P}$ scattering, we obtained a similar behavior as pp scattering, but without the pronounced dip, which was replaced instead by a broad "shoulder". Furthermore, this figure shows a comparison between the experimental and other theoretical models. In this comparison, our model calculations show good agreement with both the experimental and theoretical ones. Moreover, in order to

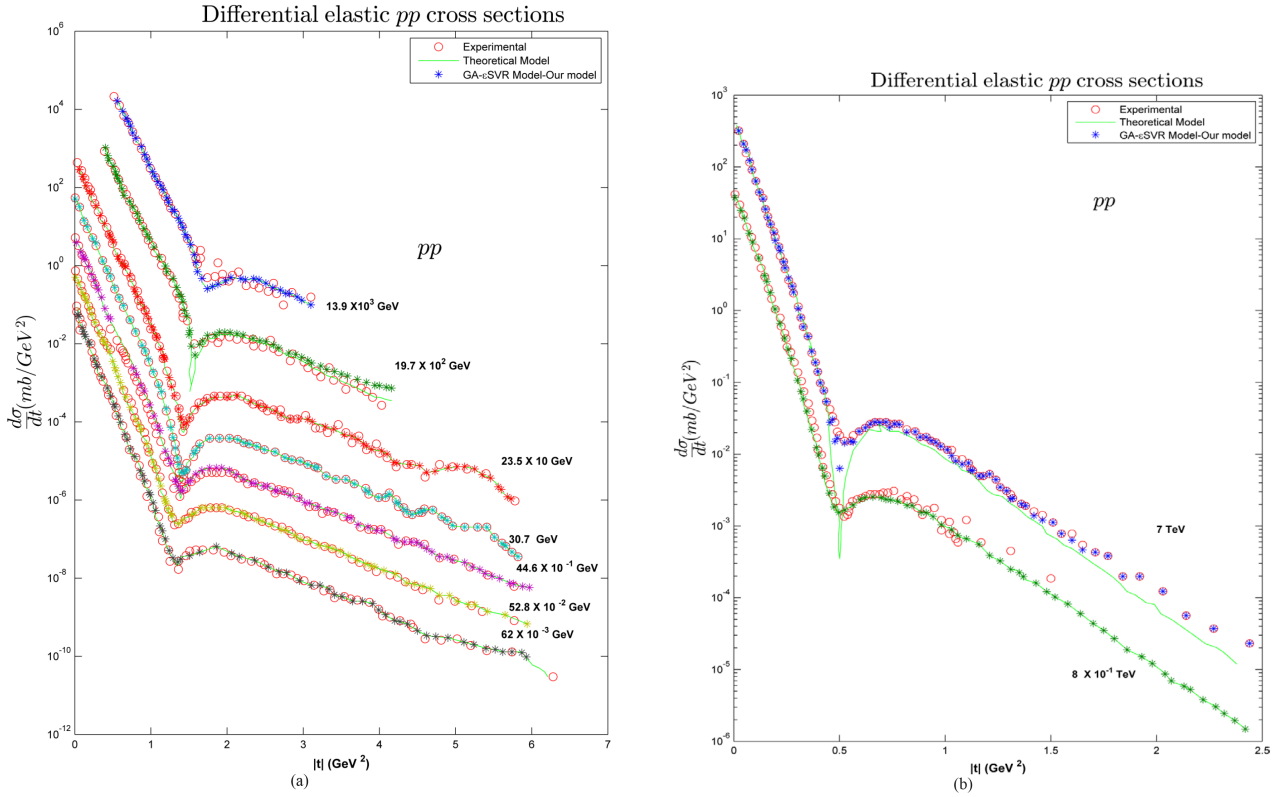

Figure 2. (a and b). $\left(\frac{d\sigma}{dt}\right)^{pp}$ of the PP as a function of the $|t|$ at different $\sqrt{s}$.(*) our GA-SVR model, experimental data (o) [11–35], and (-) theoretical ones [49,50].

evaluate the performance of the proposed GA-SVR model, the R^2 and MSE are calculated. Based on our proposed GA-εSVR model, we calculated the total cross section of PP and $P\overline{P}$,σ_{tot}. For the calculation of σ_{tot}, we first extrapolated the differential elastic cross section of each of the available data to the optical point ($|t| \to 0$) (i.e. $\frac{d\sigma}{dt}\big|_{t=0}$) . Then the optical theorem is used for the calculation of PP and $P\overline{P}$ total cross section $\sigma_{tot}^{pp,\ p\overline{p}}$ as follows:

$$\sigma_{tot}^2 = \frac{16\pi\,(\hbar c)^2}{1+\rho^2}\ \frac{d\sigma}{dt}\bigg|_{t=0}, \tag{3}$$

where $\hbar$ and c are the reduced Plank's constant and the speed of light (equal to one: $c = 1$ and $\hbar = 1$), respectively. For the ρ parameter, the COMPETE preferred-model [49] extrapolation of 0.141 ± 0.007 was chosen. Using the conversion factor, Eq. (3) becomes

$$\sigma_{tot} = 4.382 \left(\frac{d\sigma}{dt}\bigg|_{t=0}\right)^{1/2} \tag{4}$$

To calculate σ_{tot} from Eq. (4), we obtained $\frac{d\sigma}{dt}\big|_{t=0}$ for PP and $P\overline{P}$ by extrapolation of differential elastic cross sections to $|t| \to 0$ based on our GA-SVR model for the corresponding range of energy $\sqrt{s}$ =14, 23.5. 30.7, 44.6, 52.8-, 62 GeV, 7 TeV and 8 TeV,10 TeV, 13 TeV, 14 TeV for pp and $\sqrt{s}$; =13.9, 53, 546, 1800 GeV for $P\overline{P}$. A comparison is made between our results of the total cross section σ_{tot}, and the corresponding theoretical

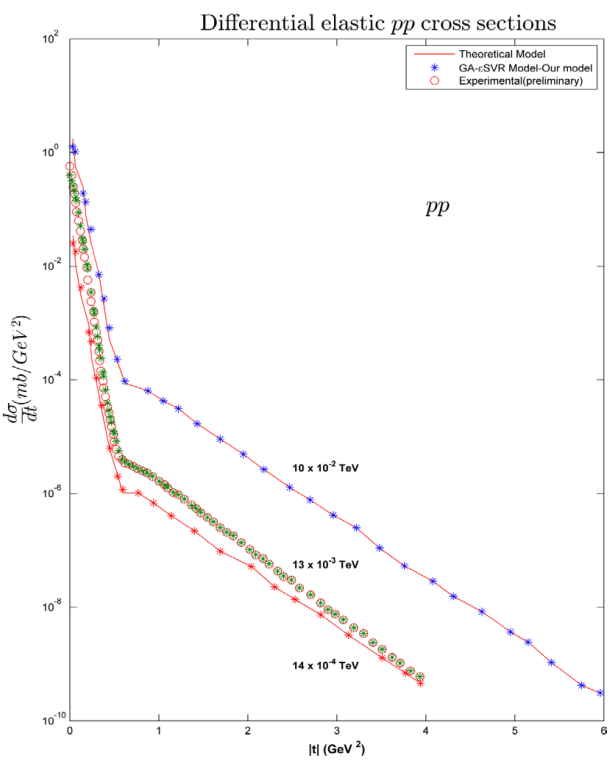

Figure 3. $\left(\frac{d\sigma}{dt}\right)^{pp}$ of the PP as a function of the $|t|$ at $\sqrt{s}$ = 10, 13, 14 TeV.

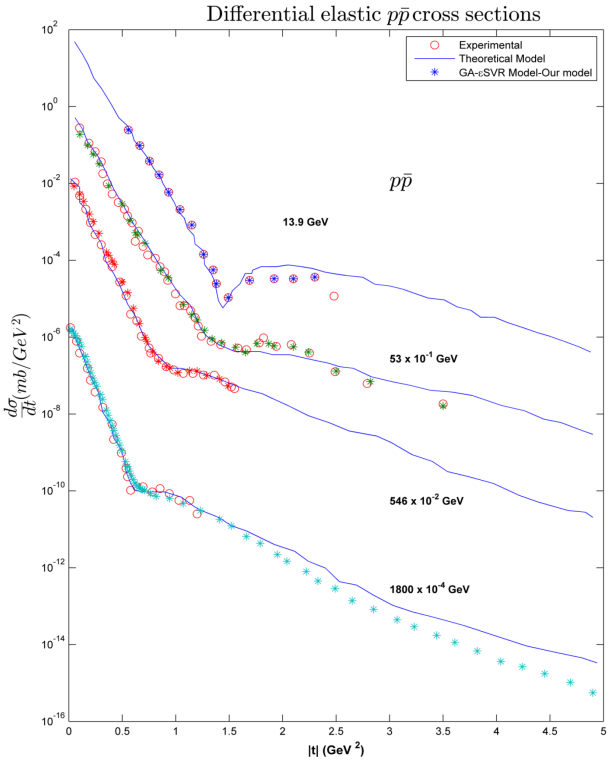

Figure 4. $\left(\frac{d\sigma}{dt}\right)^{p\bar{p}}$ of the $P\overline{P}$ as a function of the $|t|$ at different $\sqrt{s}$.(*) our GA-SVR model, experimental data (o) [11–35] and (-) theoretical ones [49,50].

and experimental ones as shown in Figure 5. This figure shows that the proposed model gives good agreement with the experimental [11-35] and theoretical [49-50] results.

4. Conclusions

In the present work, we developed and applied a hybrid computing approach GA-εSVR for the calculation and prediction of the differential elastic cross sections for PP and $P\overline{P}$ scattering, $\left(\frac{d\sigma}{dt}\right)^{pp,\,p\bar{p}}$, as well as the total cross sections $\sigma_{tot}^{pp,\,p\bar{p}}$ at various center of mass energies $\sqrt{s}$ ranging from nearly 13.9 GeV to 14 TeV in the transfer momentum squared range t = 0 to 6 GeV^2. A large data set from different labs was used to train and test the model. The proposed model reproduced well the trained experimental differential elastic cross sections, as well as the unutilized data during the training phase. Good agreement between the model predictions through the higher energies to be reached at future LHC experiment at 10 TeV, 13 TeV, and 14 TeV was obtained, as well as with other theoretical models. After the extrapolation of the available data of the differential elastic cross section in the low "t" range $\left(i.e.\ \frac{d\sigma}{dt}\Big|_{t\to 0}\right)$, a total cross section for PP and $P\overline{P}$, $\sigma_{tot}^{pp,\,p\bar{p}}$, was obtained by applying the optical theorem. The common behavior of the obtained results and the predicted ones of $\sigma_{tot}^{pp,\,p\bar{p}}$ showed a good match with the latest LHC measurements "TOTEM experiments" and the predicted ones by other models. The results of this model's calculations are very encouraging and give rise to the hope that further studies into pp and $P\overline{P}$ scattering can be conducted to describe all the particle production observables.

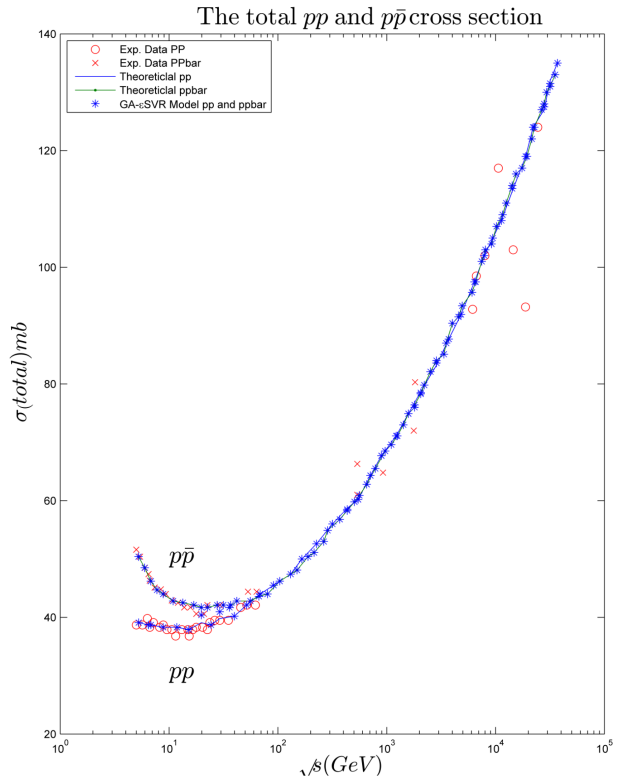

Figure 5. The total PP and $P\overline{P}$ cross section "$\sigma_{tot}^{pp,\,p\bar{p}}$".

5. Acknowledgments

The author would like to thank the Editor-in-Chief and the anonymous referees for their helpful comments and for the kind suggestions that improved the manuscript seriously.

References

[1] Siacomelli, G. *Phys. Rep.* **1976**, *23*, 123-235.

[2] Menon, M. J. *Brazn J. Phys.* **2005**, *35*,100-121.

[3] Austin, D. M.; Greiman, W. H.; Rarita, W. *Phys. Rev. D* **1970**, *2*, 2613-2627.

[4] Block M. M.; Cahn R. N. *Rev. Mod. Phys.* **1985**, *57*, 563-598.

[5] Cartiglia, N. *arXiv: hep-ex /1305.6131* (**2013**).

[6] Csorgo, T.; Glauber, R. J. *arXiv:hep-ph / 1311.2308* (**2013**).

[7] Martini, A. F. *Phys. Rev. D,* **1997**, *56*, 4338-4349.

[8] Martynov, E. *Phys. Rev. D*, **2013**, *87*, 114018-1-114018-8.

[9] Dokshitzer, Y. *Basics of Perturbative QCD*. Atlantica Séguier Frontières, 1991.

[10] Kohara, A. K.; Ferreira, E.; Kodama, T. *Eur. Phys. Jour. C* **2014**, *74*, 3175.

[11] Fagundes, D. A.; Grau, A.; Pacetti, S., Pancheri, G.; Srivastava, Y. N. *arXiv:hep-ph / 1307.0298* (**2013**).

[12] Akerlof, C. W.; Kotthaus, R.; Loveless, R. L.; Meyer, D. I.; Ambats, I.; Meyer, W. T.; Yovanovitch, D. D. *Phys. Rev. D* **1976**, *14*, 2864-2877.

[13] Breakstone, A., Crawley, H. B., Dallavalle, G. M., Doroba, K., Drijard, D., Fabbri, F.; Giacomelli, G. *Phys. Rev. Lett.* **1985**, *54*, 2180-2183.

[14] Arnison, G.; Astbury, A.; Aubert, B.; Bacci, C.; Bauer, G.; Bezaguet, A.; Calvetti, M. *Phys. Lett. B* **1983**, *128*, 336-342.

[15] Amaldi, U.; Schubert, K. R. *Nucl. Phys. B* **1980**,*166*, 301-320.

[16] Kwak, N.; Lohrmann, E.; Nagy, E.; Regler, M.; Schmidt-Parzefall, W.; Schubert, K. R.; Niebergall, F. *Phys. Lett. B* **1975**, *58*, 233-236.

[17] Amaldi, U.; Cocconi, G.; Diddens, A. N.; Dobinson, R. W.; Dorenbosch, J.; Duinker, W.; Baroncelli, A. *Phys. Lett. B* **1977**, *66*, 390-394.

[18] Baksay, L.; Baum, L., Boehm, A., Derevshikov, A., De Zorzi, G.; Giesen, H. J.; Naroska, B.; *Nucl. Phys. B* **1978**, *141*, 1-28.

[19] Nagy, E.; Orr, R. S.; Schmidt-Parzefall, W.; Winter, K.; Brandt, A.; Büsser, F. W.; Schubert, K. R. *Nucl. Phys. B* **1979**, *150*, 221-267.

[20] Battiston, R.; Bozzo, M.; Braccini, P. L.; Carbonara, F.; Carrara, R.; Castaldi, R.; Koene, B. *Phys. Lett. B* **1983**, *127*, 472-475.

[21] Kaidalov, A. B.; Poghosyan, M. G. *arXiv:hep-ph / 1109.3697*(**2011**).

[22] Bernard, D.; Bozzo, M.; Braccini, P. L.; Carbonara, F.; Castaldi, R.; Cervelli, F.; Kluit, P. *Phys. Lett. B* **1986**, *171*, 142-144.

[23] Faissler, W.; Gettner, M.; Johnson, J. R.; Kephart, T.; Pothier, E.; Potter, D.; Shahbazian, K. *Phys. Rev. D* **1981**, *23*, 33-42.

[24] Desgrolard, P.; Giffon, M.; Predazzi, E. *Z. Phys. C. Part. Fields* **1994**, *63*, 241-252.

[25] Rubinstein, R.; Baker, W. F.; Eartly, D. P.; Klinger, J. S.; Lennox, A. J.; Kalbach, R. M.; Kaplan, D. H. *Phys. Rev. D* **1984**, *30*, 1413-1432.

[26] Bozzo, M.; Braccini, P. L.; Carbonara, F.; Castaldi, R.; Cervelli, F.; Chiefari, G.; Lanzano, S. *Phys. Lett. B* **1985**, *155*, 197-202.

[27] Abe F.; Albrow M.; Amid D.; Anway-Wiese C.; Apollinari G.; Atac M.; Auchincloss P.; Ami P.; Bacchetta N.; Baden A.R.; et al. CDF Collaboration, *Phys. Rev.* **1994**, D*50*, 5518-5534.

[28] Augier, C.; Bernard, D.; Bourotte, J.; Bozzo, M.; Bueno, A.; Cases, R.; Matthiae, G. *Phys. Lett. B* **1993**, *316*, 448-454.

[29] Arnison, G.; Astbury, A.; Aubert, B.; Bacci, C.; Bauer, G.; Bezaguet, A.; Bock, R.; Bossart, R.; Bosser, J.; Bowcock, T. J. V.; et al. UA1 Collaboration: *Phys. Lett.* **1983**, *B128*, 336-342.

[30] Antchev, G.; Aspell, P., Atanassov, I.; Avati, V.; Baechler, J.; Berardi, V.; Cafagna, F. S. *Phys. Let.* **2011**, *95*, 41001-p1 41001-p7.

[31] Grafstrom, P. *Int. J. Mod. Phys. A* **2015**, *30*, 1542007-1-1542007-24.

[32] Stenzel, H. *arXiv: hep-ex/1611.02454* (**2016**).

[33] Block, M. M.; Halzen, F. *Phys. Rev. D* **2011**, *83*, 077901-1-077901-3.

[34] Islam, M. M.; Kašpar, J.; Luddy, R. J. *Mod. Phys. Lett. A* **2009**, *24*, 485-496.

[35] Nakamura, K. Particle Data Group. *J. Phys. G Nucl. Partic.* **2010**, *37*, 075021 (1422 pp).

[36] Haykin, S. Neural Networks and Learning Machines, Prentice Hall: Upper Saddle River, NJ, USA, 2008.

[37] Kiesling, C.; Zimmermann, J. (2004, December). Statistical learning methods in high-energy-and astrophysics. In Intelligent Sensors, Sensor Networks and Information Processing Conference, 2004. Proceedings of the 2004 IEEE, pp. 325.

[38] Schmidt, M.; Lipson, H. *Science* **2009**, *324*, 81-85.

[39] Whiteson, S.; Whiteson D. *Eng. Appl. Artif. Intel.* D **2009**, *22*, 1203-1217.

[40] Teodorescu, L. *IEEE T Nucl. Sci.* **2006**, *53*, 2221-2227.

[41] Akkoyun, S.; Bayram, T.; Turker, T. *Radiat. Phys. Chem.* **2014**, *96*, 186-189.

[42] El-Bakry, M. Y.; El-Dahshan, E. S. A.; El-Bakry, S. Y. *Europ. Phys. J. Plus* **2015**, *130*, 1-7.

[43] Cortes, C.; Vapnik, V. *Mach. Learn.* **1995**, *20*, 273-297.

[44] Vapnik V. N. Statistical Learning Theory. Wiley: New York, NY, USA, 1998.

[45] Vapnik, V. The Nature of Statistical Learning Theory. Springer: Berlin, Germany, 2013.

[46] Holland, J. H. Adaptation in Natural and Artificial Systems. An Introductory Analysis with Application to Biology, Control, and Artificial Intelligence. University of Michigan Press: Ann Arbor, MI, USA, 1975.

[47] Goldberg, D. E.; Holland, J. H. *Mach. Learn.* **1988**, *3*, 95-99.

[48] Bohm, G.; Zech, G. Introduction to Statistics and Measurement Analysis for Physicists. DESY: Hamburg Germany, 2010.

[49] Bourrely, C.; Soffer, J.; Wu, T. T. *Eur. J. Phys.* **2003**, C *28*, 97-105.

[50] Cudell, J. R.; Ezhela, V. V.; Gauron, P.; Kang, K.; Kuyanov, Y. V.; Lugovsky, S. B. B.; Nicolescu, E.A.; Razuvaev, N. P. *Phys. Rev. Lett.* **2002**, *89*, 201801-1-201801-4.